How to cite: *Angew. Chem. Int. Ed.* **2021**, *60*, 6408–6413
International Edition: doi.org/10.1002/anie.202015833
German Edition: doi.org/10.1002/ange.202015833

Biomimetic Glues **Hot Paper**

Accessing the Next Generation of Synthetic Mussel-Glue Polymers via Mussel-Inspired Polymerization

*Jana M. Krüger and Hans G. Börner**

Abstract: *The formation of cysteinyldopa as biogenic connectivity in proteins is used to inspire a chemical pathway toward mussel-adhesive mimics. The mussel-inspired polymerization (MIPoly) exploits the chemically diverse family of bisphenol monomers that is oxidizable with 2-iodoxybenzoic acid to give bisquinones. Those react at room temperature with dithiols in Michael-type polyadditions, which leads to polymers with thiol–catechol connectivities (TCC). A set of TCC polymers proved adhesive behavior even on challenging poly(propylene) substrates, where they compete with commercial epoxy resins in dry adhesive strength. MIPoly promises facile scale up and exhibits high modularity to tailor adhesives, as proven on a small library where one candidate showed wet adhesion on aluminum substrates in both water and sea water models.*

Different marine invertebrates like, for example, tube worms, sea cucumbers, or mussels, show remarkable wet adhesion and in some aspects outperform highly optimized synthetic adhesives.[1] In particular, the gluing system of marine mussels has provided inspiration for decades and the underlying biochemistry was largely revealed in the meantime.[2] The adhesive apparatus was described as an injection molding process, where purpose-adapted mussel foot proteins (mfps) are secreted in a concerted manner, forming byssus threads and adhesive plugs.[3] L-3,4-Dihydroxyphenylalanin (Dopa) with its catechol moiety is central for adhesion and cohesion,[4] but the sequence environment of Dopa and other specific adhesion sequence motifs are also relevant.[2c,5]

This made Dopa and synthetic catechol analogs the basis of a rich family of mussel-inspired polymers.[6] For instance, catechol-presenting polymers reach impressive adhesive properties under both dry and wet conditions[7] or provide anchors for robust surface coatings.[6b] The versatile chemistry of catechols enabled covalent or non-covalent cross-linking, leading to, for example, robust coatings or hydrogels.[9] Recently, a mussel-inspired polymerization (MIPoly) of peptides was described, taking advantage of the Michael-acceptor properties of oxidized Dopa residues.[10] In AB-type unimers, dopaquinone residues (A) react smoothly with thiols of cysteine residues (B) forming the adhesive cysteinyldopa connectivities. Dopaquinones were accessed either from tyrosine residues by tyrosinase[10,11] or from Dopa residues by, for example, periodate oxidation.[12] MIPoly was demonstrated on i. sequence derivatives of the consensus sequence of mfp-1 (**AKPSYPPTYK**GGGC),[10] ii. different fusion peptides with pH-responsive or Zn^{2+}-ion activatable β-sheet forming domains for cohesion control,[13] and iii. minimal adhesive domains **YK**C.[12] The resulting artificial mfps exhibit thiol–catechol connectivities (TCCs) in the backbone, show fast adsorption from aqueous solutions onto various substrates, and the coatings resist hypersaline conditions as found in the Dead Sea. Some artificial mfps reach adhesive energies of up to 10.9 mJ m^{-2}, they coat even fluoropolymer surfaces and show adherence under 599 mM NaCl sea water model conditions.[10,12]

Peptide-based artificial mfps offer a facile implementation of folding propensities to control cohesion[13] and enable tailormade interactions by exploiting material specific adsorption domains as found by combinatorial means.[5a,c,14] However, the potential of peptide- or protein-based artificial mfps for commodity applications might be limited by cost-intensive scale up.

Herein, we expand the MIPoly process to access a class of fully synthetic adhesive polymers, relying on a technically available commodity monomer platform (Figure 1) and avoiding the utilization of peptides or enzymes. The modular AA + BB strategy uses bisquinones (AA-type) to react with dithiols (BB-type), leading to synthetic TCC polymers, which exhibit thiol–catechol connectivities to address adhesion and cohesion.

In the chemically activated, mussel-inspired polymerization of catechol/thiol-bearing peptides (AB-type), the catechol oxidation and the disulfide formation are competing reaction pathways.[12] Apparently, disulfide bridge formation seems to be not dominating during polymerization of, for example, Dopa-Xaa-Cys tripeptides. However, potential difficulties can be circumvented by separating the catechol oxidation from the polymerization step. Therefore, bisquinone (AA-type) and dithiol (BB-type) monomers were introduced, where the former was synthesized prior to the polymerization (Scheme 1). It is intriguing that the full enzymatic reaction of tyrosinase oxidation from phenol via *ortho*-catechol to *ortho*-quinone can be synthetically conducted in a one-pot reaction with 2-iodoxybenzoic acid (IBX).[15] This enables utilization of bisphenol A and the

[*] J. M. Krüger, Prof. H. G. Börner
Laboratory for Organic Synthesis of Functional Systems Institution Department of Chemistry, Humboldt-Universität zu Berlin
Brook-Taylor-Strasse 2, 12489 Berlin (Germany)
E-mail: h.boerner@hu-berlin.de
Supporting information and the ORCID identification number(s) for the author(s) of this article can be found under: https://doi.org/10.1002/anie.202015833.

chemically diverse set of bisphenol monomers that is available for large scale production of epoxy resins or polycarbonates.

The IBX oxidation of bisphenol A (BPA) is highly suited for monomer synthesis as bisquinone A (BQA) precipitates in high yield in form of a reddish solid from the reaction mixture, not requiring further purification (S.I. Section S4.1). It should be noted that BPA is categorized as substance of concern because of its endocrine disrupting properties, and urgent research is demanded to realize biofriendly alternatives not only for MIPoly but also for epoxy resins or poly(carbonate)s. However, the pool of bisphenol monomers is readily available in large scale for a proof of concept and includes less suspicious monomer structures with reduced adverse effects. In further studies, the introduced MIPoly might be expanded to biofriendly or biobased monomer alternatives.

A solution polymerization was carried out by combining the isolated AA-type BQA with 1 equiv. of the BB-type monomer 2,2′-(ethylenedioxy)diethanethiol (EDET, Scheme 1). After the addition of the dithiol, the color of the polymerization mixture changed within a few minutes from dark red to pale yellow, indirectly suggesting a rapid consumption of the quinones (Figure 2a, S.I. Figure S5). Polar solvents, such as NMP, DMF, or DMSO, were found to favor the reaction and gel permeation chromatography (GPC) proved the formation of TCC polymers at room temperature within approximately 15 minutes (S.I. Figure S6). As is typical for polyaddition reactions, the raw products contained low molecular mass fractions, which were assigned to cyclization products by liquid chromatography mass spectrometry (S.I. Figure S7). For instance, UPLC-ESI-MS (negative mode) shows the presence of cyclic dimers with m/z 437 $[(AA\text{-}BB)_1{}^c\text{-}H]^-$ and cyclic tetramers with m/z 875 $[(AA\text{-}BB)_2{}^c\text{-}H]^-$. Easy purification is feasible by precipitation into aqueous methanol to yield circa 60% polymers (S.I. Figure S8). GPC indicates that the molecular weights of the isolated products depend on monomer concentration. While a polymerization with 22.6 g L^{-1} (BQA/NMP) yields polymers that have molecular weights of $M_{w,app.} = 8.9$ kDa ($Đ = 1.5$) with distributions reaching up to 40 kDa, an increase to concentrations of 100 g L^{-1} (BQA/NMP) leads to polymers with $M_{w,app.} =$ 15.2 kDa with distributions of $Đ = 2.4$, reaching values of up to 100 kDa (Figure 2b).

MALDI-TOF MS shows the homologous row of mass signals with alternating peak distances that correspond to AA- and BB-monomer masses of up to $(AA–BB)_7$ repeats (Figure 2c). Defects originating from disulfide bridges, e.g. $[BB]_n$-repeats, were not evident, confirming that this pathway is negligible. This is consistent with tributyl phosphine top-up experiments, where the addition of reducing agents to cleave disulfide bonds in TCC polymers had no dramatic effect on GPC traces (S.I. Figure S18). The formation of TCC structures as dominating polymerization pathway was ultimately proven by a MALDI-TOF MS/MS analysis. Fragmentation of the hexamer species ($[(AA\text{-}BB)_3 + Na]^+$ at m/z 1337.34) provides typical fragments indicative of the thiol-substituted catechols (Figure 2d, S.I. Section S5.5). ^{1}H NMR proved the stoichiometric ratio between AA and BB monomers present

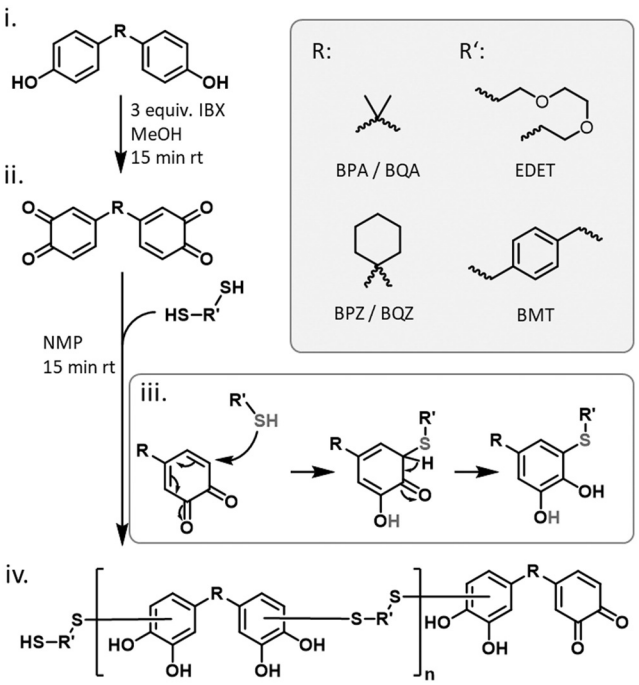

Scheme 1. The reaction pathway of MIPoly: Bisphenols (i) can be oxidized by IBX to yield bisquinones (ii) that react in a Michael-type polyaddition (iii) to TCC polymers (iv).

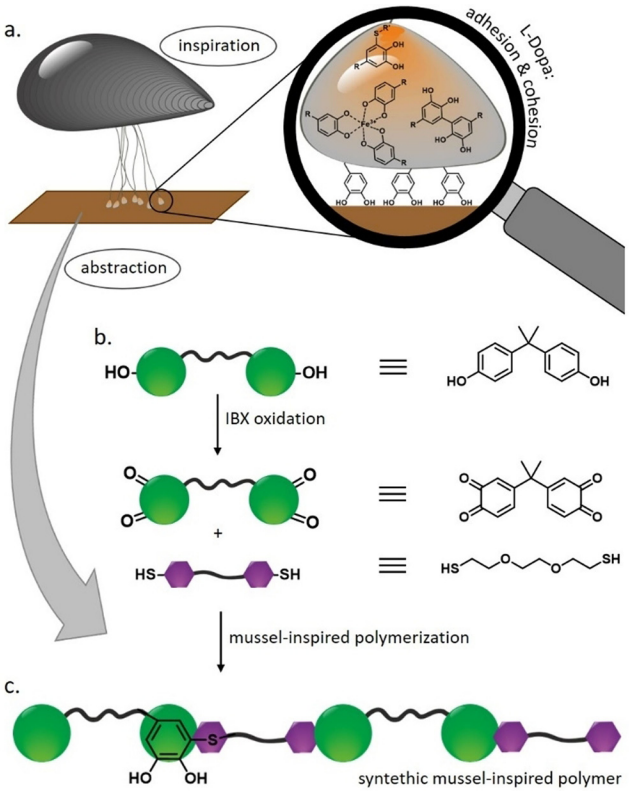

Figure 1. The mussel-inspired polymerization abstracts a biogenic reaction of dopaquinone and cysteine to give cysteinyldopa connectivities as observed, for example, in green mussels[16] (a). Rebuilding the mechanism based on bisphenol monomers, which were oxidized by IBX to yield bisquinones to react with dithiols (b) and provide adhesive TCC polymers with thiol–catechol connectivities (c).

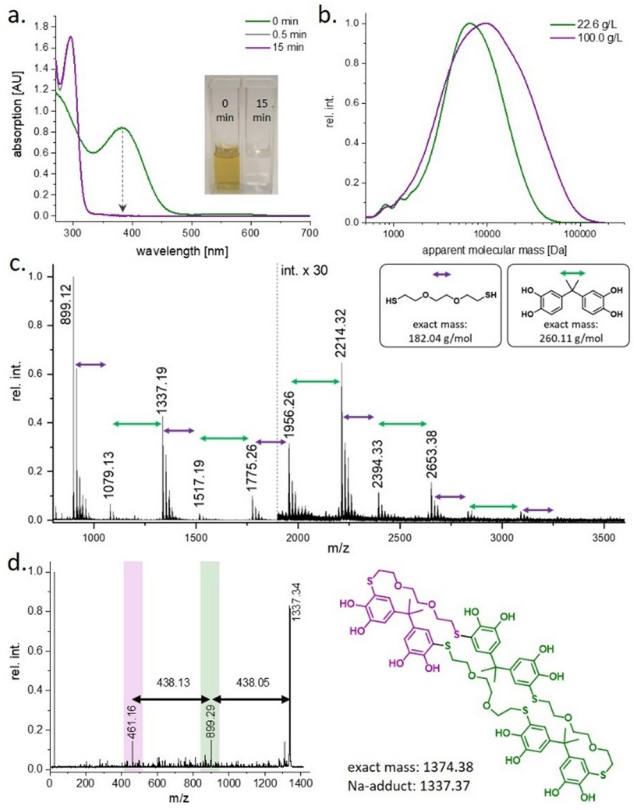

Figure 2. MIPoly of BQA/EDET: UV/Vis spectroscopy indicates rapid consumption of BQA (a). GPC shows polymer formation (b) and MALDI-TOF MS proves the [AA-BB]$_n$ structure by showing alternating monomer mass distances (c). MALDI-TOF MS/MS confirmed the TCC structure by providing characteristic fragments of the hexamer (d).

in purified polymers (S.I. Figure S11). Moreover, ^{1}H–^{13}C HSQC and ^{1}H–^{13}C HMBC confirmed the identity of the thiol–catechol connectivities (S.I. Section S5.7). Interestingly, the regioselectivity of the Michael-type addition in the MIPoly proceeds close to that of low molecular weight reactions[17] and leads to 5′- to 2′-substituted isomers with ratios of 2.4:1.

Further insight into the MIPoly of BQA and EDET was provided by kinetic investigations. UPLC–ESI MS monitored a remarkably fast consumption of BQA from an equimolar AA + BB polymerization mixture, which occurred within less than 30 seconds (S.I. Figure S7). GPC analysis proved the formation of polymer products to be finished within the first 2 min as no changes in GPC traces were evident within the following 4 h (S.I. Figure S17). This was consistent with the fast disappearance of quinones that was followed by UV/Vis spectroscopy at 386 nm (Figure 2a).[18] Under the given conditions, a reliable monitoring of the reaction kinetics was difficult as reaction times were close to mixing times. Even for 100-times diluted polymerization mixtures, 50% BQA was consumed after 30 seconds and 90% was reached within approx. 7 min (S.I. Figure S16). It is noteworthy that the MIPoly of synthetic monomers proceeds similarly fast compared to the enzyme-activated polymerization of peptides in water.[10]

The MIPoly proved to be very robust as the copolymerization of BQA/EDET proceeded in NMP in a temperature window from 0 °C to 180 °C (S.I. Figure S19). The reaction was performed in air and tolerates water contents of up to circa 1% (S.I. Figure S20).

The MIPoly process of bisquinones and dithiols seems to be generic and can be expanded to other dithiols as well as to the set of technical bisphenols. For instance, a TCC polymer with decreased backbone flexibility was accessed by employing 1,4-benzenedimethanethiol (BMT) and bisquinone Z (BQZ), which was available from bisphenol Z by IBX oxidation (S.I. Section 4.2). The stoichiometric mixture of BQZ and BMT reacts rapidly in NMP, requiring approx. 15 min until no changes were evident in the GPC (S.I. Figure S21). To prove modularity, the two bisquinones (BQA&BQZ) and the two dithiols (EDET&BMT) were scrambled, leading to a library of four different TCC polymers. The MIPoly was carried out with c[BQ] = 0.5 mol L^{-1} at 1:1 monomer ratio to yield the set of TCC polymers [p(BQA-EDET) $M_{w,app.} = 15.9$ kDa ($Đ = 2.6$), p(BQA-BMT) $M_{w,app.} = 11.5$ kDa ($Đ = 2.6$), p(BQZ-EDET) $M_{w,app.} = 20.7$ kDa ($Đ = 3.4$) and p(BQZ-BMT) $M_{w,app.} = 19.0$ kDa ($Đ = 3.8$); S.I. Figure S22]. Obviously, BQZ leads to polymers with higher apparent molecular weights. This was explained based on GPC trace analysis, suggesting that the conformationally less flexible BQZ/BMT reduce the tendency to form low molecular weight cycles compared to BQA/EDET (S.I. Figure S23, S24).

After successful synthesis the material properties of the set of TCC polymers were analyzed. All polymers have excellent thermal stabilities and show related maxima in degradation rates within 320–350 °C (S.I. Figure S25). The glass transition temperature (T_g) is one important parameter in adhesive design and differential scanning calorimetry (DSC) revealed that T_g depends on the chemical structure of the TCC polymers. As expected, the flexible ether segment of EDET dominates T_g of p(BQA-EDET) and p(BQZ-EDET) to give 66 °C and 81 °C. The rigid aromatic BMT increased T_g for both p(BQA-BMT) and p(BQZ-BMT) to circa 105 °C, and in those TCC polymers the BQ component was less relevant (S.I. Figure S26).

To investigate the adhesive properties of the set of TCC polymers as "hot-melt"-like glues, shear tests at room temperature were performed on aluminum and poly(propylene) (PP) substrates (Figure 3, S.I. Section S6). The force–extension curves on aluminum show one sharp fraction event (Figure 3b), while samples on PP often present stepwise failure, starting at the edges and progressing to the center (Figure 3b and S.I. Figure S31).

Interestingly, even in the small library, distinct preferences were evident with respect to achievable adhesive strength on specific materials (Figure 3c). On aluminum, BQA-based polymers p(BQA-EDET) and p(BQA-BMT) reach adhesive strengths of 2.5 ± 0.7 MPa and 2.4 ± 0.7 MPa, while the BQZ-family p(BQZ-EDET) and p(BQZ-BMT) provides 1.1 ± 0.3 MPa and 1.2 ± 0.5 MPa. On PP substrates the EDET ether segment is of importance as adhesion strengths for p(BQZ-EDET) and p(BQA-EDET) reach 1.7 ± 0.2 MPa and 1.2 ± 0.2 MPa, whereas the BMT-family p(BQA-BMT) and

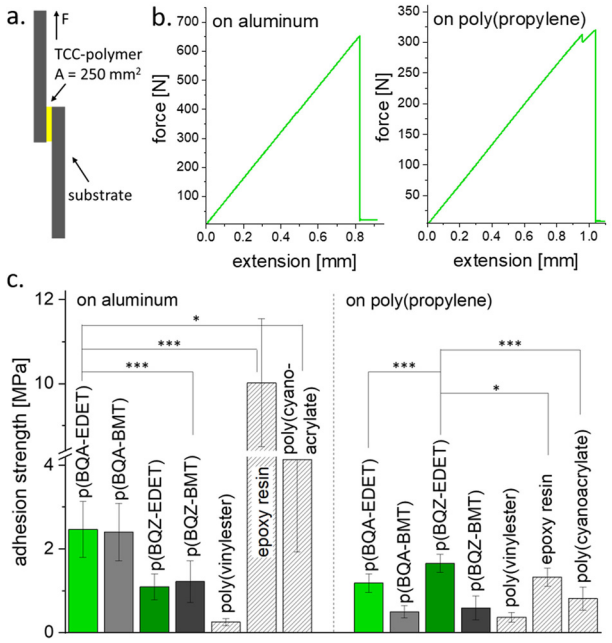

Figure 3. Adhesive shear tests on TCC polymers: Schematic shear test setting (a) and representative force–extension curves (b). Adhesion properties of TCC polymers p(BQA-EDET), p(BQA-BMT), p(BQZ-EDET), and p(BQZ-BMT) as well as of controls with commercial glues on aluminum and PP substrates (c, statistical significance determined by t-test (Student)).

p(BQZ-BMT) shows 0.5 ± 0.1 MPa and 0.6 ± 0.3 MPa. In general, the TCC polymers with EDET tend to reach the highest adhesion strengths for both substrates. This might suggest suitable interaction capabilities of the ether with the surfaces, but could also result from lower T_g.

It is not surprising that the highest adhesive strengths were found on aluminum. Nonetheless, the gluing of PP as a low surface energy material that is challenging to adhere to was indeed remarkable. The relevant binding modes of polymers to PP substrates are still under debate. Börner et al. recently reported on phage display with next-generation sequencing, suggesting that, counterintuitively, van der Waals interactions are not necessarily dominating adhesion on PP.[5a]

Despite reaching notable adhesive strength on PP, TCC polymers cope better with polar substrates. This was concluded from the fact that under the given conditions, all the observed failure modes on PP substrates were dominantly adhesive in nature, while failures on aluminum mainly show a cohesive nature (S.I. Figure S28, S30). The differing failure characteristics on aluminum and PP also explained the observed effects of the adhesive performance on the molecular weight of TCC glues. To reveal this finding systematically, a set of p(BQA-EDET) was synthesized, exhibiting different molecular weights ($M_{w,app} = 4.0$ kDa, $Đ = 1.8$; $M_{w,app} = 9.0$ kDa, $Đ = 1.6$ and $M_{w,app} = 15.9$ kDa, $Đ = 2.6$). Lap shear tests indicated an increase of the adhesive strengths with increased molecular weight on both substrates (S.I. Section S6.2). Stronger effects on aluminum were found where cohesion was the limiting factor. In contrast to this, PP samples show adhesive failure modes, making the cohesion improvement by higher molecular weights less effective.

Comparing the adhesive performance of TCC polymers with that of commercial poly(vinyl ester), poly(cyanoacrylate), or 2K-epoxide glues reveals competitive or even slightly higher adhesive strengths that can be reached with TCC polymers on difficult PP (Figure 3c). On PP, epoxy resin glue reaches adhesive strengths of 1.3 ± 0.2 MPa and performs better than non-cross-linked poly(vinyl ester) and poly(cyanoacrylate) glues. It is noteworthy that the non-optimized p(BQZ-EDET) and p(BQA-EDET) were able to compete very well with epoxy glue on PP, as they reach adhesive strengths of 1.7 ± 0.2 MPa and 1.2 ± 0.2 MPa, respectively. On the polar surfaces of aluminum, the p(BQA-EDET) and p(BQA-BMT) provide adhesive strengths of 2.5 ± 0.7 MPa and 2.4 ± 0.7 MPa, which are fairly below poly(cyanoacrylate) superglue (4.1 ± 2.2 MPa) but outranged by the epoxy glue, which is, however, a 3D-crosslinked resin (10.0 ± 1.5 MPa). The commercial poly(vinyl ester) glue fails on both aluminum and PP substrates and reached 0.4 ± 0.1 MPa, the lowest strength in this set.

Considering the well-established binding behavior of catechols on metal oxide surfaces, a strong adhesion of TCC polymers on aluminum can be expected. This is consistent with the dominantly observed cohesive failure of TCC polymers on aluminum, which indicates that adhesion is apparently not the limiting factor. Cohesion in TCC polymers might be improved by the utilization of tri- or multivalent thiols to access 3D-cross-linked resins. Moreover, metal-ion-induced cross-linking might enhance the cohesion of these glues, as it was described for mussel-inspired hydrogels.[19]

In addition to the adhesion tests using dry "hot-melt" curing under pressure, underwater adhesion performance was also studied. Following the protocol of Wilker et al.,[7e] a TCC polymer solution in chloroform was deposited under water onto aluminum substrates. After placing the second substrate on top, curing took place underwater for 3 days at 50 °C and lap shear tests were performed at 21 °C after taking the specimens out of the water.

From the TCC-adhesive library, only p(BQZ-EDET) showed sufficient solubility in chloroform, enabling underwater glue application in pure water as well as in 599 mM NaCl sea water equivalents (S.I. Section 6.3). Interestingly, p(BQZ-EDET) proved similar adhesive capabilities in both water and sea water model solution, reaching adhesive strengths of 0.4 ± 0.3 MPa and 0.4 ± 0.2 MPa, respectively. Considering that the adhesive strength under water is often reduced compared to dry glue settings, it is noteworthy that p(BQZ-EDET) still reaches circa 40 % strength under wet conditions compared to that under dry "hot-melt"-like gluing. Apparently, water does not seem to dramatically affect the adhesive performance, and curing under soft conditions might offer room for optimization. This was indicated by control experiments, where p(BQZ-EDET) was deposited onto dry aluminum substrates followed by 3 days of dry curing at 50 °C. Under those conditions, adhesive strengths of 0.2 ± 0.1 MPa were found, which are within the experimental error in a comparable range to the wet experiments. It should be noted that, already from the very small TCC compound library, p(BQZ-EDET) was identified, which exhibits underwater adhesive strength in the range of literature-known

synthetic mussel-inspired polymers. For instance, Wilker et al.[7e] reported wet adhesive strengths of 0.2 ± 0.1 MPa for adhesives with higher molecular weights of $M_w = 84$ kDa on comparable aluminum substrates, which nonetheless reached outstanding 3.0 ± 0.4 MPa on polished aluminum.

In summary, a synthetic pathway of the mussel-inspired polymerization (MIPoly) was shown, which relied on the industrially available bisphenol (BPx) monomer class, which was oxidized to bisquinones (BQx) by 2-iodoxybenzoic acid (IBX). Those AA-type monomers smoothly react with dithiols (BB-type) to result in polymers with adhesive thiol–catechol connectivities (TCC). The robust polymerization proceeds by rapid Michael-type polyaddition, which enables polymerization of bisquinone A (BQA) with 2,2′-(ethylenedioxy)diethanethiol (EDET) within approx. 15 min at room temperature. The TCC structures were verified by MALDI-TOF MS/MS and 2D-NMR. The modularity of the MIPoly was shown by extending the monomer pool with bisquinone Z (BQZ) and 1,4-benzenedimethanethiol (BMT). The adhesive properties of the resulting TCC polymer library were investigated on aluminum and PP substrates. Ultimately, adhesive strengths of 2.5 MPa on aluminum and 1.7 MPa on PP were reached. PP gluing is known to be challenging, but the non-optimized p(BQZ-EDET) adhesive already outcompetes not-preprimed commercial epoxy resin glues. Additionally, p(BQZ-EDET) proved wet adhesion strengths of 0.4 MPa on aluminum substrates in both water and sea water equivalents, which compete with dry controls under similar curing conditions. The modular approach of the MIPoly enables the facile synthesis of TCC polymer libraries and might promise the combination of computational predictive tools with automatized synthesis platforms to tailor next-generation wet adhesives.

Acknowledgements

The authors thank D. Auhl, O. Löschke, and P. Wang (TU Berlin) for fruitful discussions and shear tests of poly(cyanoacrylate) and 2K-epoxide glue on aluminum and DSC measurements. We thank H. Stephanowitz and F. Liu (Leibniz Institute for Molecular Pharmacology, Buch) for MALDI-TOF MS/MS, A. Dallmann (HU Berlin) for 2D-NMR, and B. Kobin (HU Berlin) for TGA analysis. Financial support was received from the German Chemical Industry Association (Verband der Chemischen Industrie; Kekulé excellence stipend, No. 102551) and the German Research Foundation DFG/BO1762/9-2. Open access funding enabled and organized by Projekt DEAL.

Conflict of interest

The authors declare no conflict of interest.

Keywords: adhesive library · Biomimetic adhesives · Dopa mimics · Mussel-inspired glue

[1] a) M. Almeida, R. L. Reis, T. H. Silva, *Mater. Sci. Eng. C* **2020**, *108*, 110467; b) E. Hennebert, B. Maldonado, P. Ladurner, P. Flammang, R. Santos, *Interface Focus* **2015**, *5*, 20140064.

[2] a) B. P. Lee, P. B. Messersmith, J. N. Israelachvili, J. H. Waite, *Annu. Rev. Mater. Res.* **2011**, *41*, 99–132; b) J. H. Waite, *J. Exp. Biol.* **2017**, *220*, 517–530; c) N. L. Venkatareddy, P. Wilke, N. Ernst, J. Horsch, A. Dallmann, M. Weber, H. G. Börner, *Adv. Mater. Interfaces* **2019**, *6*, 1900501.

[3] a) J. H. Waite, *Int. J. Adhes. Adhes.* **1987**, *7*, 9–14; b) F. Jehle, E. Macías-Sánchez, P. Fratzl, L. Bertinetti, M. J. Harrington, *Nat. Commun.* **2020**, *11*, 1696.

[4] a) J. H. Waite, M. L. Tanzer, *Science* **1981**, *212*, 1038–1040; b) H. Lee, N. F. Scherer, P. B. Messersmith, *Proc. Natl. Acad. Sci.* **2006**, *103*, 12999–13003.

[5] a) C. Juds, J. Schmidt, M. G. Weller, T. Lange, U. Beck, T. Conrad, H. G. Börner, *J. Am. Chem. Soc.* **2020**, *142*, 10624–10628; b) V. Samsoninkova, N. L. Venkatareddy, W. Wagermaier, A. Dallmann, H. G. Börner, *Soft Matter* **2018**, *14*, 1992–1995; c) S. Große, P. Wilke, H. G. Börner, *Angew. Chem. Int. Ed.* **2016**, *55*, 11266–11270; *Angew. Chem.* **2016**, *128*, 11435–11440.

[6] a) P. Kord Forooshani, B. P. Lee, *J. Polym. Sci. Part A* **2017**, *55*, 9–33; b) J. L. Dalsin, B.-H. Hu, B. P. Lee, P. B. Messersmith, *J. Am. Chem. Soc.* **2003**, *125*, 4253–4258; c) M. Yu, T. J. Deming, *Macromolecules* **1998**, *31*, 4739–4745; d) P. Wilke, H. G. Börner, *ACS Macro Lett.* **2012**, *1*, 871–875; e) Q. Wei, K. Achazi, H. Liebe, A. Schulz, P. L. M. Noeske, I. Grunwald, R. Haag, *Angew. Chem. Int. Ed.* **2014**, *53*, 11650–11655; *Angew. Chem.* **2014**, *126*, 11834–11840.

[7] a) B. K. Ahn, S. Das, R. Linstadt, Y. Kaufman, N. R. Martinez-Rodriguez, R. Mirshafian, E. Kesselman, Y. Talmon, B. H. Lipshutz, J. N. Israelachvili, J. H. Waite, *Nat. Commun.* **2015**, *6*, 8663; b) A. Li, Y. Mu, W. Jiang, X. Wan, *Chem. Commun.* **2015**, *51*, 9117–9120; c) B. D. B. Tiu, P. Delparastan, M. R. Ney, M. Gerst, P. B. Messersmith, *Angew. Chem. Int. Ed.* **2020**, *59*, 16616–16624; *Angew. Chem.* **2020**, *132*, 16759–16767; d) M. G. Mazzotta, A. A. Putnam, M. A. North, J. J. Wilker, *J. Am. Chem. Soc.* **2020**, *142*, 4762–4768; e) M. A. North, C. A. Del Grosso, J. J. Wilker, *ACS Appl. Mater. Interfaces* **2017**, *9*, 7866–7872.

[8] a) A. Thomas, H. Bauer, A.-M. Schilmann, K. Fischer, W. Tremel, H. Frey, *Macromolecules* **2014**, *47*, 4557–4566; b) H. Watanabe, A. Fujimoto, R. Yamamoto, J. Nishida, M. Kobayashi, A. Takahara, *ACS Appl. Mater. Interfaces* **2014**, *6*, 3648–3653; c) P. Wilke, N. Helfricht, A. Mark, G. Papastavrou, D. Faivre, H. G. Börner, *J. Am. Chem. Soc.* **2014**, *136*, 12667–12674.

[9] a) D. W. R. Balkenende, S. M. Winkler, P. B. Messersmith, *Eur. Polym. J.* **2019**, *116*, 134–143; b) A. Andersen, M. Krogsgaard, H. Birkedal, *Biomacromolecules* **2018**, *19*, 1402–1409; c) N. Holten-Andersen, M. J. Harrington, H. Birkedal, B. P. Lee, P. B. Messersmith, K. Y. C. Lee, J. H. Waite, *Proc. Natl. Acad. Sci.* **2011**, *108*, 2651–2655; d) Q. Wei, R. Haag, *Mater. Horiz.* **2015**, *2*, 567–577; e) H. Lee, S. M. Dellatore, W. M. Miller, P. B. Messersmith, *Science* **2007**, *318*, 426–430.

[10] J. Horsch, P. Wilke, M. Pretzler, M. Seuss, I. Melnyk, D. Remmler, A. Fery, A. Rompel, H. G. Börner, *Angew. Chem. Int. Ed.* **2018**, *57*, 15728–15732; *Angew. Chem.* **2018**, *130*, 15954–15958.

[11] J. Horsch, P. Wilke, H. Stephanowitz, E. Krause, H. G. Börner, *ACS Macro Lett.* **2019**, *8*, 724–729.

[12] J. M. Kohn, J. Riedel, J. Horsch, H. Stephanowitz, H. G. Börner, *Macromol. Rapid Commun.* **2020**, *41*, 1900431.

[13] a) S. Arias, S. Amini, J. Horsch, M. Pretzler, A. Rompel, I. Melnyk, D. Sychev, A. Fery, H. G. Börner, *Angew. Chem. Int. Ed.* **2020**, *59*, 18495; *Angew. Chem.* **2020**, *132*, 18653; b) S. Arias, S. Amini, J. M. Krüger, L. D. Bangert and H. G. Börner, *Soft Matter*, **2021**, https://doi.org/10.1039/D0SM02118K.

[14] a) A. Care, P. L. Bergquist, A. Sunna, *Trends Biotechnol.* **2015**, *33*, 259 – 268; b) K. A. Gunay, H. A. Klok, *Bioconjugate Chem.* **2015**, *26*, 2002 – 2015; c) T. Schwemmer, J. Baumgartner, D. Faivre, H. G. Börner, *J. Am. Chem. Soc.* **2012**, *134*, 2385 – 2391; d) F. Hanßke, E. Kemnitz, G. H. Börner, *Small* **2015**, *11*, 4303 – 4308.
[15] R. Bernini, M. Barontini, F. Crisante, M. C. Ginnasi, R. Saladino, *Tetrahedron Lett.* **2009**, *50*, 6519 – 6521.
[16] H. Zhao, J. H. Waite, *Biochemistry* **2005**, *44*, 15915 – 15923.
[17] S. Ito, G. Prota, *Experientia* **1977**, *33*, 1118 – 1119.
[18] M. Yu, J. Hwang, T. J. Deming, *J. Am. Chem. Soc.* **1999**, *121*, 5825 – 5826.
[19] a) H. M. Siebert, J. J. Wilker, *ACS Sustainable Chem. Eng.* **2019**, *7*, 13315 – 13323; b) M. H. Kim, J. N. Lee, J. Lee, H. Lee, W. H. Park, *ACS Biomater. Sci. Eng.* **2020**, *6*, 3103-3113; c) X. Sha, C. Zhang, M. Qi, L. Zheng, B. Cai, F. Chen, Y. Wang, Y. Zhou, *Macromol. Rapid Commun.* **2020**, *41*, 2000055; d) S. Li, N. Chen, Y. Li, J. Zhao, X. Hou, X. Yuan, *Macromol. Mater. Eng.* **2020**, *305,* 1900620.

Manuscript received: November 27, 2020
Revised manuscript received: January 15, 2021
Accepted manuscript online: January 28, 2021
Version of record online: February 12, 2021

